

Full paper / Mémoire

Reversible photomagnetic properties of the molecular compound $[\{\text{Cu}^{\text{II}}(\text{bipy})_2\}_2\{\text{Mo}^{\text{IV}}(\text{CN})_8\}] \cdot 9\text{H}_2\text{O} \cdot \text{CH}_3\text{OH}$

Corine Mathonière^{a,*}, Hirokazu Kobayashi^b, Rémy Le Bris^a,
Abdellah Kaïba^a, Isabelle Bord^c

^a Université Bordeaux-1, CNRS, Institut de chimie de la matière condensée de Bordeaux, UPR9048, 87, avenue du Docteur-Albert-Schweitzer, 33608 Pessac cedex, France

^b Faculty of Engineering, Kyushu University, 744 Motoooka, Nishi-ku, Fukuoka 819-0385, Japan

^c Laboratoire IMS-UMR 5218 CNRS, ENSEIRB-Université Bordeaux-1, 351, cours de la Libération, 33405 Talence, France

Received 8 October 2007; accepted after revision 7 January 2008

Available online 4 March 2008

Abstract

The optical and photomagnetic properties of $[\{\text{Cu}^{\text{II}}(\text{bipy})_2\}_2\{\text{Mo}^{\text{IV}}(\text{CN})_8\}] \cdot 9\text{H}_2\text{O} \cdot \text{CH}_3\text{OH}$ (**1**) have been reinvestigated. A comparison between spectra in solution and in the solid state revealed the presence of an intervalence band (or Metal–Metal Charge Transfer, hereafter noted MMCT) at 570 nm. The photomagnetic properties have been performed in a Superconducting QUantum Interference Device at 10 K with irradiation in the range of the MMCT: 488 nm, 520 nm and 647 nm at 10 K. An important increase of the magnetic signal has been measured after 1 h of irradiation at 488 nm, whereas a weaker increase has been obtained for the irradiation at 520 nm in the same conditions. Moreover, after an excitation at 488 nm, an irradiation at 647 nm has induced a decrease of the magnetic moment, which corresponds to a partial deexcitation. The complete characterization of the photoproduct has been realised after an irradiation of 4 h at 488 nm. The photomagnetic properties have shown an increase of the paramagnetism of **1** at low temperature. After a thermal heating at 300 K, the material goes back to its initial state before irradiation. It is the first time that a fully reversible photomagnetic behaviour for the compound $[\{\text{Cu}^{\text{II}}(\text{bipy})_2\}_2\{\text{Mo}^{\text{IV}}(\text{CN})_8\}] \cdot 9\text{H}_2\text{O} \cdot \text{CH}_3\text{OH}$ has been described. The observed properties have been discussed in terms of an electron transfer mechanism $\text{Mo} \rightarrow \text{Cu}$. **To cite this article:** C. Mathonière et al., C. R. Chimie 11 (2008).

© 2008 Académie des sciences. Published by Elsevier Masson SAS. All rights reserved.

Résumé

Les propriétés optiques et photomagnétiques de $[\{\text{Cu}^{\text{II}}(\text{bipy})_2\}_2\{\text{Mo}^{\text{IV}}(\text{CN})_8\}] \cdot 9\text{H}_2\text{O} \cdot \text{CH}_3\text{OH}$ (**1**) ont été réinvestiguées. Une étude comparative de spectres en solution et à l'état solide a révélé la présence d'une bande d'intervalence (ou transfert de charge métal–métal, noté par la suite MMCT) à 570 nm. Les propriétés photomagnétiques ont été mesurées à l'aide d'un Superconducting QUantum Interference Device en irradiant le composé à 488 nm, à 520 nm et 647 nm à 10 K. Une augmentation importante du signal magnétique a été mesurée pour une heure d'irradiation à 488 nm, tandis qu'une augmentation plus faible a été observée à 520 nm. De plus, après une excitation à 488 nm, une irradiation à 647 nm a conduit à une décroissance du moment magnétique, correspondant à une désexcitation partielle. La caractérisation complète du photoproduit a été réalisée après une irradiation à 488 nm de 4 h. Les propriétés photomagnétiques montrent une augmentation du paramagnétisme du composé à basse température.

* Corresponding author.

E-mail address: mathon@icmcb-bordeaux.cnrs.fr (C. Mathonière).

Après chauffage à 300 K, le matériau revient dans son état magnétique original, avant irradiation. C'est la première fois qu'un comportement photomagnétique réversible est décrit pour le composé $[\{\text{Cu}^{\text{II}}(\text{bipy})_2\}_2\{\text{Mo}^{\text{IV}}(\text{CN})_8\}] \cdot 9\text{H}_2\text{O} \cdot \text{CH}_3\text{OH}$. Les propriétés observées sont discutées dans le cadre d'un mécanisme de transfert de charge $\text{Mo} \rightarrow \text{Cu}$. **Pour citer cet article :** C. Mathonière et al., C. R. Chimie 11 (2008).

© 2008 Académie des sciences. Published by Elsevier Masson SAS. All rights reserved.

Keywords: Coordination compounds; Octacyanomolybdate; Electron transfer; Magnetism; Photomagnetism

Mots-clés : Composés de coordination ; Octacyanomolybdate ; Transfert électronique ; Magnétisme ; Photomagnétisme

1. Introduction

Bimetallic cyanides have attracted considerable interest in the molecular chemistry community because of their unusual electronic and magnetic properties. The Prussian blue analogues forming three-dimensional networks with general formula $(\text{Cat})_x\text{M}_y[\text{M}'(\text{CN})_6]$ (Cat standing for an alkali metal; M and M' for a 3d transition metallic ion) were the first compounds to exhibit very interesting properties, as for example magnets above room temperature [1,2], and switchable properties. The switching of magnetic properties has been induced by the application of various external stimuli: temperature [3], light [4–8], pressure [9,10] and current [11] in a reversible way. Later, new bimetallic two- or three-dimensional networks built from octacyanomolybdate precursors $[\text{M}'(\text{CN})_8]^{n-}$, M' being a 4d or 5d metallic ion, have also shown switchable properties [12–15]. These switchable materials have been identified as mixed-valence systems with the existence of a Metal–Metal Charge Transfer band (noted hereafter as MMCT), conferring a strong colour to the materials. Then, the switching mechanism is associated with an internal electron transfer between the different metallic centres. This photomagnetic functionality opens some interesting perspectives in magnetic data storage.

The coordination chemistry of the anionic hexacyanomolybdate $[\text{M}'(\text{CN})_6]^{n-}$ or octacyanomolybdate $[\text{M}(\text{CN})_8]^{n-}$ precursors, is rather close. Both give rise to a variety of bimetallic molecular compounds, from discrete molecules, chains, 2D and 3D networks [16–20]. Interestingly, molecules built from $[\text{M}(\text{CN})_8]^{n-}$ are today the rare ones to exhibit photomagnetic properties [13,21,22]. The molecular nature of these systems is crucial for future devices, because of their solubility in common solvents and then of their easy shaping.

In the present work, we would like to complete the study of one of these molecular systems, namely $[\{\text{Cu}^{\text{II}}(\text{bipy})_2\}_2\{\text{Mo}^{\text{IV}}(\text{CN})_8\}] \cdot x\text{Solv.}$, Solv. being water and/or methanol molecules. In our previous paper [21], we presented the synthesis, structural, and

magnetic characterization of $[\{\text{Cu}^{\text{II}}(\text{bipy})_2\}_2\{\text{Mo}^{\text{IV}}(\text{CN})_8\}] \cdot 5\text{H}_2\text{O} \cdot \text{CH}_3\text{OH}$. Its structure consists of a neutral trinuclear molecule in which a central $[\text{Mo}(\text{CN})_8]^{4-}$ is linked to two $[\text{Cu}(\text{bipy})_2]^{2+}$ through cyanide bridges (Fig. 1, inset). The compound behaves as a paramagnet since the Mo^{IV} ion is diamagnetic ($4d^2$, $S = 0$) and the magnetism comes from the peripheral Cu^{2+} ions ($3d^9$, $S = 1/2$) that are too far away from each other to interact through exchange interactions. The photomagnetic behaviour of the compound has been investigated using a UV irradiation (337–356 nm), and revealed an irreversible change in magnetic properties. This behaviour contrasts with properties of other cyano-bridged $\text{Cu}^{\text{II}}-\text{Mo}^{\text{IV}}$ compounds that have been characterized later. All show a Metal–Metal Charge Transfer band in the 413–480-nm range. When they are irradiated with light in the MMCT energy range, they show reversible magnetic changes [12–15]. The photomagnetic behaviour in these systems has been attributed to a photo-induced charge transfer in Cu–Mo pairs, changing the valence state of each pair, from Cu^{II} ($3d^9$, $S = 1/2$)– Mo^{IV} ($4d^2$, $S = 0$) to Cu^{I} ($3d^{10}$, $S = 0$)– Mo^{V} ($4d^1$, $S = 1/2$). In this work, we decided to study again the photomagnetic behaviour of $[\{\text{Cu}^{\text{II}}(\text{bipy})_2\}_2\{\text{Mo}^{\text{IV}}(\text{CN})_8\}] \cdot x\text{Solv.}$ in order to obtain reversible photomagnetism. In particular, the choice of the wavelength used for photoexcitation is examined in detail to generate a reversible photomagnetic behaviour of **1** under visible-light irradiation.

2. Experimental

The precursors $\text{K}_4[\text{Mo}^{\text{IV}}(\text{CN})_8] \cdot 2\text{H}_2\text{O}$ and $\text{Cu}(\text{bipy})_2\text{Cl} \cdot \text{Cl}$ were prepared according to the literature [23,24]. Green crystals of **1** were obtained by slow diffusion in water in an H-shaped tube of one 10 mL aqueous solution containing 0.25×10^{-4} mol of $\text{K}_4[\text{Mo}^{\text{IV}}(\text{CN})_8] \cdot 2\text{H}_2\text{O}$ and one 10 mL mixture of water/methanol (50/50) containing 0.25×10^{-4} mol of $\text{CuCl}_2 \cdot 5\text{H}_2\text{O}$ and 0.5×10^{-4} mol of bipyridine. After one month, green crystals were collected, and washed with water. CHNS

microanalysis was performed on a ThermoElectron Flash EA1112. The elemental analysis confirmed that the formula is $[\{\text{Cu}(\text{bipy})_2\}_2\{\text{Mo}(\text{CN})_8\}]\cdot 9\text{H}_2\text{O}\cdot \text{CH}_3\text{OH}$ (**1**). Calcd: C, 47.08; H, 4.35; N, 17.9. Found: C, 47.05; H, 4.27; N, 16.8.

The crystals were not good enough for complete X-ray structure determination. The room-temperature powder X-ray diffraction pattern was recorded over the angular range $5^\circ < 2\theta < 110^\circ$ with a 0.02° step and a counting time of 10 s on a Philips PW 3040/00 X'Pert MPD device in Bragg–Brentano geometry using diffracted beam graphite monochromator Cu $K\alpha$ irradiation ($\lambda = 1.5406 \text{ \AA}$). Unit cell parameter values were derived from a peak indexation using DICVOL91 [25].

The optical properties were investigated with a CARY 5E spectrometer equipped with a diffuse reflectance sphere. The solution and solid-state spectra have been collected at room temperature.

The magnetic properties were determined using an MPMS-5S Quantum Design SQUID (Superconducting QUantum Interference Device) magnetometer operating with an external magnetic field of 0.5 T within the range of 2–300 K. Photoexcitations were performed using a Spectrum Physics Series 2025 mixed gas Ar/Kr laser ($\lambda = 488 \text{ nm}$, 520 nm, 647 nm) coupled via an optical fibre to the cavity of an MPMS-5S Quantum Design SQUID magnetometer. Without light irradiation, the measurements have been obtained on a polycrystalline sample of 14.26 mg. For these experiments, the magnetic data were corrected for the diamagnetic contribution of the sample holder (plastic bag) and the diamagnetic contribution of the sample using Pascal constants. The photomagnetic experiments were performed on a 1.1-mg polycrystalline sample maintained in half gelatin capsule allowing the sample to be directly positioned at about 2.5 cm from the optical fibre. Due to the weak mass of the sample, the SQUID centring derives significantly with the temperature. In order to correct the SQUID signal, the data have been corrected measuring the sample before irradiation and comparing the data with the measurements done on 14.26 mg of sample (see above). The deduced empirical correction has been applied to all the measurements of an experimental set of data. However, the points measured between 60 K and 110 K are not presented because they correspond to the measure of a very weak magnetic signal with a large experimental uncertainty, the weakness of the magnetic signal being due to the almost exact compensation of the paramagnetic contribution of the sample and to the diamagnetic contribution of the sample holder and the sample.

3. Results

3.1. X-ray powder diffraction

The X-ray diffraction powder pattern of **1** is shown in Fig. 1, and it is compared to the already reported crystal structure of $[\{\text{Cu}^{\text{II}}(\text{bipy})_2\}\{\text{Mo}^{\text{IV}}(\text{CN})_8\}]\cdot 5\text{H}_2\text{O}\cdot \text{CH}_3\text{OH}$ [21]. The X-ray diffraction pattern of $[\{\text{Cu}^{\text{II}}(\text{bipy})_2\}\{\text{Mo}^{\text{IV}}(\text{CN})_8\}]\cdot 5\text{H}_2\text{O}\cdot \text{CH}_3\text{OH}$ has been simulated from the atomic positions and unit cell dimensions (from the atomic positions and unit cell dimensions ($a = 11.3006(4) \text{ \AA}$, $b = 12.0886(5) \text{ \AA}$, $c = 22.9589(9) \text{ \AA}$, $\alpha = 81.799(2)^\circ$, $\beta = 79.787(2)^\circ$, $\gamma = 62.873(2)^\circ$, $V = 2740.3 \text{ \AA}^3$, $P\bar{1}$) contained in the Crystallographic Information File. For **1**, the best solution to index the well-defined peaks (9 peaks) in the $8\text{--}12^\circ$ range gives the triclinic cell $P\bar{1}$, with $a = 11.706(5) \text{ \AA}$, $b = 12.250(8) \text{ \AA}$, $c = 22.171(13) \text{ \AA}$, $\alpha = 65.57(4)^\circ$, $\beta = 94.06(6)^\circ$, $\gamma = 93.71(6)^\circ$, and $V = 2886 \text{ \AA}^3$. The similarity of the two patterns suggests that **1** retains the architecture in a trimetallic molecule where the molybdenum ion is connected through cyanide bridges to two $\{\text{Cu}(\text{bipy})_2\}$ sites.

3.2. Optical spectroscopy

The absorption spectrum in the solid state of **1** is shown in Fig. 2 in the 400–800-nm range. For comparison, the spectra of the precursors $\text{K}_4[\text{Mo}^{\text{IV}}(\text{CN})_8]\cdot 2\text{H}_2\text{O}$ and $\text{Cu}(\text{bipy})_2\text{Cl}\cdot \text{Cl}$ are also given. The Mo precursor presents a band below 470 nm, which is

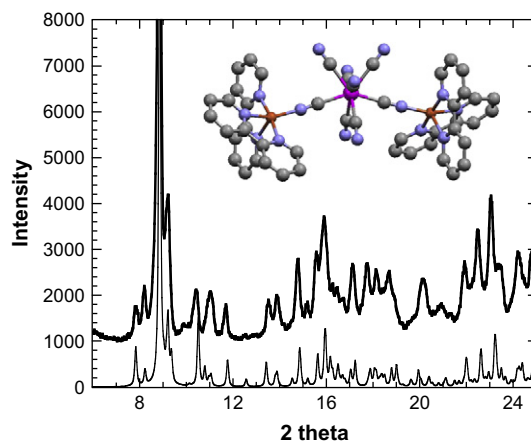


Fig. 1. X-ray powder diffractogram (—) for **1** and the diffractogram simulated from the crystal structure of $[\{\text{Cu}^{\text{II}}(\text{bipy})_2\}\{\text{Mo}^{\text{IV}}(\text{CN})_8\}]\cdot 5\text{H}_2\text{O}\cdot \text{CH}_3\text{OH}$ (---). Inset: the crystal structure of $[\{\text{Cu}^{\text{II}}(\text{bipy})_2\}\{\text{Mo}^{\text{IV}}(\text{CN})_8\}]\cdot 5\text{H}_2\text{O}\cdot \text{CH}_3\text{OH}$. Red: copper atoms, pink: molybdenum, grey: carbon atoms, and blue: nitrogen atoms (for interpretation of the references to colour in this figure legend, the reader is referred to the web version of this article).

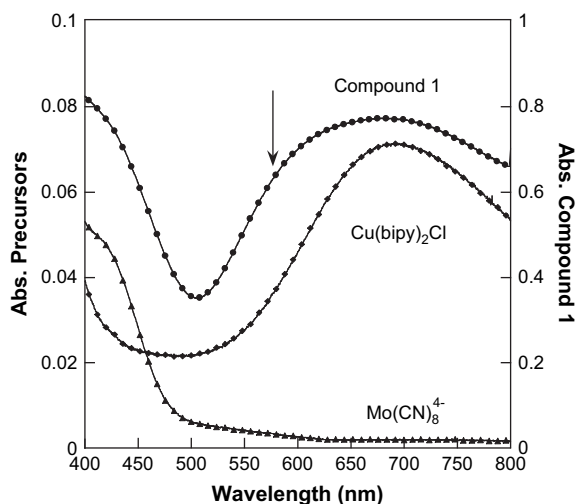


Fig. 2. Solid-state optical spectra of **1** (●), and its precursors: $[\text{Cu}(\text{bipy})_2]^{2+}$ (◆) and $[\text{Mo}(\text{CN})_8]^{4-}$ (▲).

attributed to a d–d transition of the Mo ion [26]. The Cu precursor presents a large band, with a maximum at ca. 700 nm, which is attributed to d–d transitions of the Cu^{2+} ion [27]. In **1**, these two absorption bands are present due to the existence of these chromophores in the molecule. Additionally, a dissymmetry appears in the spectrum of **1** around 570 nm (marked by an arrow in Fig. 2). This new feature could be attributed to a Metal–Metal Charge-Transfer (MMCT) band, or to a distortion of the Cu site, due to the substitution of the chloro anion by the cyano anion in the coordination surrounding of copper ion. At this stage of the study, it is impossible to decide unambiguously the best attribution for this spectral feature.

To propose a correct assignment of this optical feature, we realised the following experiment suggested by Henning et al. [28] in solution. To a yellow aqueous solution of 5×10^{-4} M of $\text{K}_4[\text{Mo}(\text{CN})_8] \cdot 2\text{H}_2\text{O}$ is added a blue aqueous solution of 5×10^{-4} M of $[\text{Cu}(\text{bipy})_2]\text{Cl} \cdot \text{Cl}$. An immediate change of colour from yellow to green is observed. In the final solution, the system consists of 1:1 associate, namely a Cu:Mo pair. The absorption spectra of the two solutions before addition and the final solution after addition are plotted in Fig. 3. The change of colour is then clearly identified as a new absorption feature at 540 nm. To isolate this feature, a difference spectrum has been calculated using the mathematical difference as: $\text{Abs}(\text{K}_4[\text{Mo}(\text{CN})_8]_{\text{solution}}) - \text{Abs}([\text{Cu}(\text{bipy})_2]\text{Cl}_{\text{solution}})$ (see Fig. 3). The difference spectrum shows a component at 530 nm. It shows that the spectrum of the Cu:Mo pair is not simply the sum of the spectra of its

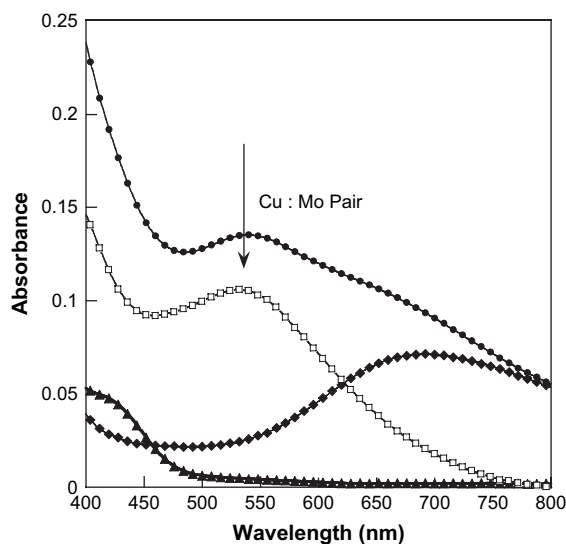


Fig. 3. Aqueous solution optical spectra of the Cu:Mo pair (●), $[\text{Cu}(\text{bipy})_2]\text{Cl}_2$ (◆) and $[\text{Mo}(\text{CN})_8]^{4-}$ (▲), and the difference spectrum (□, see text).

components. If it were the case, the difference spectrum should be close to zero in absorbance. Therefore the new band at 530 nm is associated with an MMCT band in the Cu:Mo pair. This MMCT band is associated with an electron transfer between the donor Mo and the acceptor Cu as $\text{Cu}^{2+}:\text{Mo}^{4+} \rightarrow \text{Cu}^+:\text{Mo}^{5+}$ [28]. Let us now compare the spectra of the Cu:Mo pair in solution and **1** in the solid state. Before comparison, note that **1** corresponds to a different stoichiometry 2Cu:Mo. Then the absorption at ca. 700 nm for **1** is more important in intensity than in the Cu:Mo pair. But the new feature at ca. 570 nm appearing as a shoulder in Fig. 2 (marked by the arrow) is close to the MMCT band in the pair. Therefore, we propose the MMCT attribution for the band around 570 nm for **1**. For comparison, the 3D network $[\{\text{Cu}(\text{H}_2\text{O})_2\}_2\{\text{Mo}(\text{CN})_8\}] \cdot 4\text{H}_2\text{O}$ exhibits an MMCT at 480 nm. The red shift between the 3D network and **1** may be attributed to a different coordination sphere of the Cu^{2+} site that induces a change in the redox potential of the acceptor site. Note that in our previous study of **1** [21], we did not identify the MMCT band because of its large overlap with d–d transitions of the Cu^{2+} sites. The present in-solution study of the precursors is then very helpful to discriminate the different spectral contributions.

3.3. Magnetic and photomagnetic properties

The photomagnetic investigations consist of the study of the magnetism of a material in the solid state before and after light excitation. The selection of the

wavelength of the irradiation is important because we have already observed two types of photomagnetic behaviours for octacyanometalates, depending on the wavelengths used for excitation. For compounds exhibiting MMCT transitions in their optical spectra, the irradiation is performed in an energy range close to the MMCT [8,12–15]. The objective of these studies is to photo-induce an electron transfer between the two metallic sites involved in the MMCT band. The change in oxidation states of the metal centres accompanying the electron transfer may change the exchange interactions, and then the magnetism. For compounds without MMCT band, it has been shown that few octacyanometalate bimetallic systems are photomagnetically active species when irradiated with UV irradiation [22]. The change in magnetism has been shown to be irreversible, and was attributed to the oxidation change of the $\text{Mo}^{\text{IV}}(\text{CN})_8$ core. On the contrary, in these studies, the reduced species have not been identified clearly.

With our experimental set-up based on a mixed gas Ar/Kr laser, we tested three different wavelengths for **1**, covering the MMCT energy range: 488 nm, 520 nm and 647 nm. As reported for the 3D network $[\{\text{Cu}(\text{H}_2\text{O})_2\}_2\{\text{Mo}(\text{CN})_8\}] \cdot 4\text{H}_2\text{O}$ [12], the first two wavelengths corresponding to higher energy than MMCT may induce an increase of the magnetic moment, whereas the third one (with energy smaller than MMCT) is expected to induce a decrease of the magnetic moment. The compound has been irradiated directly in the SQUID chamber at 10 K during one or several hours. The results reported in Table 1 correspond to a complete photoexperiment with 7 different runs to test the photosensitivity of the compound. The 488-nm line induces an important increase of the magnetic moment (Run 1 immediately followed by Run 2). After Run 2, the photoproduct has been fully characterized (see description in next paragraph). During the characterization, the sample has been warmed up to 300 K. When placing again at 10 K after this thermal treatment, **1** recovers

its original χT product. Then, it is possible to use the 488-nm line again for a new population (Run 3). This experiment shows that the process can be repeated. Moreover, after one irradiation with 488-nm wavelength, we used the 647-nm line in order to test the photoreversibility (Run 6). Actually, this sequence induces an increase of the magnetic moment of **1** under 488 nm, followed by a decrease of it under 647 nm. Finally, we compared the 488-nm and 520-nm lines during 1 h of irradiation. Both induce an increase of the magnetic moment (+17% and +6%, respectively), with a better efficiency of the 488-nm line. This long photomagnetic experiment shows the repeatability of the photo-induced changes and the reversible magnetic changes under light irradiation.

Let us describe now the magnetic characterization and the photomagnetic properties after Run 2 described above. First, the magnetic properties of **1** before irradiation are summarized in Fig. 4 in the form of χT vs. T plots, where χ is the molar paramagnetic susceptibility and T the temperature. At room temperature, the χT product is $0.78 \text{ cm}^3 \text{ K/mol}$.

When the temperature is lowered, the χT product at 5000 Oe is almost constant down to 60 K and then slowly decreases to reach the minimum of $0.775 \text{ cm}^3 \text{ K/mol}$ at 1.8 K. Fit of the experimental data to Curie–Weiss law above 2 K leads to the following Curie and Weiss constants: $0.782 \text{ cm}^3 \text{ K/mol}$ and -0.17 K , respectively. The Curie constant is in agreement with the expected value ($0.75 \text{ cm}^3 \text{ K/mol}$) for the presence of two Cu(II) ($S = 1/2$, $C = 0.375 \text{ cm}^3 \text{ K/mol}$ with $g_{\text{Cu}} = 2$). The negative Weiss constant suggests the presence of very weak antiferromagnetic interactions between spin carriers as expected from the crystal structure that shows that all the spin centres are separated by diamagnetic NC–Mo(IV)–CN bridges. The magnetization versus field at 2 K (Fig. 5) is very close to the sum of two Brillouin functions with $S = 1/2$ with $g = 2$, with a value of $1.8 \text{ N}\beta$ at 50 kOe.

Table 1
Photoexcitation experiment with different runs performed at 10 K in the SQUID magnetometer ($H = 5 \text{ kOe}$) for **1**

Run	Laser beam, λ/nm	Time of irradiation	Evolution of EMU	Variation of EMU	Remarks
1	488	1 h	Increase	+17%	
2 (After 1)	488	4 h	Increase	+90% (From 1)	Full characterization and relaxation
3	488	2 h	Increase	+25%	
4	647	1 h 30 min	Decrease	-10%	
5	488	1 h	Increase	+15%	
6	647	1 h	Decrease	-6%	
7	520	1 h	Increase	+6%	

The different runs have been performed in continuity on the same sample.

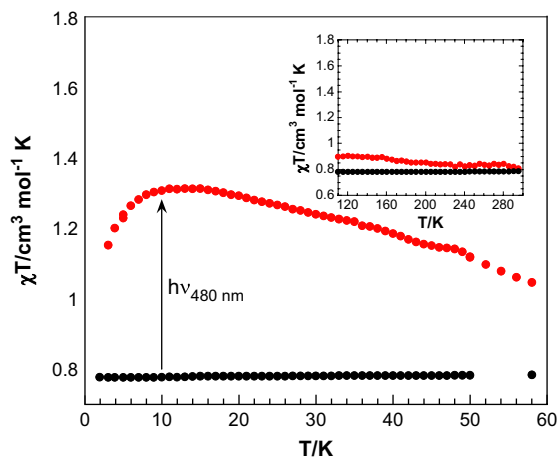


Fig. 4. Thermal dependence of the χT product for **1**, before irradiation (\bullet), and after irradiation (\bullet) in the 2–60-K range. In inset is shown the 110–300-K range.

Then the sample was irradiated at 10 K for 4 h (Runs 1 and 2, Table 1), and was characterized further in the dark. After 4 h of irradiation, an important increase of the χT product at 10 K has been measured from $0.78 \text{ cm}^3 \text{ K/mol}$ to $1.31 \text{ cm}^3 \text{ K/mol}$. This corresponds to a 62% increase of the magnetism at 10 K. It has been checked that the magnetic signal after irradiation at 10 K is stable for half an hour. This stability renders possible the further study of the photoproduct: first in the low-temperature region, and then when the material is warming up. Fig. 5 shows magnetization versus field at 2 K after irradiation. If the shape of the curve after irradiation is similar to the magnetization before irradiation, the values are bigger in all the field range. For example, the value at 50 kOe is $2.29 \text{ N}\beta$, and corresponds to a 27% increase compared to the magnetization before irradiation ($1.8 \text{ N}\beta$). Clearly, the photoproduct has a higher magnetic moment than the material before irradiation. This result is confirmed with the χT vs. T plot after irradiation, in the 2–60 K range. When the temperature is increased, the χT product first increases till a plateau between 10 K and 20 K at $1.31 \text{ cm}^3 \text{ K/mol}$, and then shows a smooth decrease at higher temperatures to reach a value at 60 K of $1.05 \text{ cm}^3 \text{ K/mol}$. At 110 K, the χT product is $0.9 \text{ cm}^3 \text{ K/mol}$, and when the temperature is further increased, a gentle decrease continues to recover the χT value before irradiation around $0.8 \text{ cm}^3 \text{ K/mol}$ near 230 K. Finally, above 230 K, there is almost no difference between the χT product after and before irradiation. After the thermal treatment at 300 K of the material, we measured again

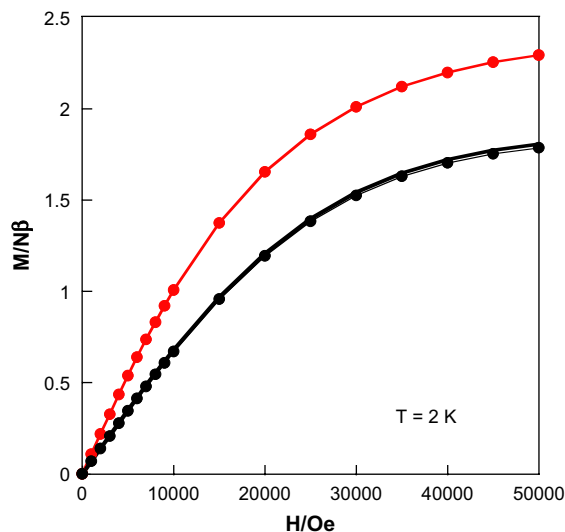


Fig. 5. Field dependence of the magnetization at 2 K for **1**, before irradiation (\bullet), after irradiation (\bullet), and after thermal treatment at 300 K (\bullet).

the magnetization at 2 K. The result is a curve that is completely superimposed to the curve obtained before irradiation. These magnetic data confirm that the process is fully reversible.

4. Discussion and conclusion

In this work, we reinvestigate the optical and photomagnetic properties of the trinuclear bimetallic compound $[\{\text{Cu}^{\text{II}}(\text{bipy})_2\}\{\text{Mo}^{\text{IV}}(\text{CN})_8\}]\cdot 9\text{H}_2\text{O}\cdot \text{CH}_3\text{OH}$ in order to find a wavelength range for photoexcitation which induces a reversible photomagnetic behaviour. By comparison with other Cu–Mo compounds, reversible photomagnetic changes have been observed when the systems are irradiated in the range of the MMCT band observed in their optical spectra. Then, the first part of our study was the identification of an MMCT band in **1**. This identification is difficult due to the big overlap between d–d transitions of the Cu^{2+} and an eventual MMCT band. We have used the method of the difference between the spectrum of **1** and those obtained for the different precursors present in the bimetallic compound. This analysis has given the appearance of a new band in the trimetallic compound at 570 nm, which we have assigned to the MMCT band. Then, the compound has been irradiated in the range of the MMCT band. A fully reversible photomagnetic behaviour has been obtained. This reversibility of the magnetic properties is very important, because it is one of the criteria for this type of systems to be used as active component in devices.

In the literature, the energy range and the reversibility of the photomagnetic process offer enough guarantees to affirm that a photo-induced electron transfer is responsible for the observed effects. In the Cu–Mo systems, the electron transfer is realised in Cu:Mo pair, where Mo acts as the donor of one electron, and Cu as the acceptor of one electron. Note that only the reduction of the copper sites has been identified with spectroscopic methods in the 3D CuMo network [29]. The magnetic properties of $[\{\text{Cu}^{\text{II}}(\text{bipy})_2\}_2\{\text{Mo}^{\text{IV}}(\text{CN})_8\}] \cdot 9\text{H}_2\text{O} \cdot \text{CH}_3\text{OH}$ after irradiation may be analysed within an electron transfer between Mo and Cu ions. Before irradiation, the compound behaves as the triad $\text{Cu}^{\text{II}}\text{Mo}^{\text{IV}}\text{Cu}^{\text{II}}$, which corresponds to an $S = 1/2 - S = 0 - S = 1/2$ triad. The measured magnetic properties are in agreement with this scheme. During irradiation, an electron transfer occurs in a Cu:Mo pair, and finally converts the compound into the triad $\text{Cu}^{\text{II}}\text{Mo}^{\text{V}}\text{Cu}^{\text{I}}$ or an $S = 1/2 - S = 1/2 - S = 0$ triad. The effect of the electron transfer in the triad is not to change the spins present in it, but only the localisation of the spins. Before irradiation, the two spins of $1/2$ are separated by the diamagnetic bent NC–Mo–CN bridge (9.79 Å, 141°) [21]. After irradiation, the same spins of $1/2$ are only separated by the diamagnetic CN bridges (5.2 Å). This last situation can generate exchange interactions. The higher magnetic moment measured after irradiation may be the result of ferromagnetic interactions between Cu^{II} and Mo^{V} ions. For a system of two spins of $1/2$, ferromagnetic interactions lead to a gap between a triplet ground state with a spin of $S = 1$ and a singlet spin state $S = 0$. In this analysis, the plateau of χT between 10 K and 20 K would correspond to the complete population of the triplet state. This is also in agreement with the magnetization curves at 5 K and 2 K, which can be fitted with Brillouin function of a spin state $S = 1$ and a value of 2.28 for the Zeeman g factor. Above 20 K, the decrease of the χT can be viewed as the depopulation of the triplet state with respect to the singlet state, but also as a combined effect with the relaxation to the dark state. To be valid, this explanation implies an energy gap Δ between the triplet state and the singlet state of about $+40 \text{ cm}^{-1}$.¹ This value seems to be relatively high, but it has been already measured for $\text{Cu}^{\text{II}}\text{—NC—W}^{\text{V}}$ systems [30]. To explain the further decrease of χT below 10 K, additional anti-ferromagnetic interactions between molecules would be operative. The interpretation of charge transfer from

Mo to Cu induced by light seems correct to explain the observed photomagnetism. Nevertheless, to validate the charge transfer mechanism, a spectroscopic signature of the oxidation of the Mo site and the reduction of the Cu site is necessary. We plan in the future ESR and X-ray studies of **1** under light irradiation. Finally, the fit of the thermal dependence of the χT plot is difficult because the relaxation behaviour (that is to say the return of the system in its original state) is not known. The time dependence of χT after irradiation for several temperatures is necessary to characterize the relaxation behaviour. This work is under progress.

To sum up, we have studied for the first time the reversible magnetic changes under a blue-light irradiation of the molecular compound $[\{\text{Cu}^{\text{II}}(\text{bipy})_2\}\{\text{Mo}^{\text{IV}}(\text{CN})_8\}] \cdot 9\text{H}_2\text{O} \cdot \text{CH}_3\text{OH}$. The light irradiation induces an increase of the magnetic moment of the compound. The reversibility is fully obtained by a thermal treatment at 300 K, and partially obtained with the use of a red light. Up to now, this system is the second one in the octacyanomolybdate chemistry to exhibit reversible photomagnetic properties.

Acknowledgements

The authors would like to thank the Aquitaine Region for supporting the photomagnetic platform. This work was also supported by a Grant-in-Aid for HK named “Integration Technology of Mechanical Systems for Hydrogen Utilization” from the Ministry of Education, Culture, Science, Sports and Technology (MEXT) of Japan.

References

- [1] S. Ferlay, T. Mallah, R. Ouhaes, P. Veillet, M. Verdagner, *Nature* 378 (1995) 701.
- [2] S. Holmes, G.S. Girolami, *J. Am. Chem. Soc.* 121 (1999) 5593.
- [3] W. Kosaka, K. Nomura, K. Hashimoto, S.-I. Ohkoshi, *J. Am. Chem. Soc.* 127 (2005) 8590.
- [4] O. Sato, T. Iyoda, A. Fujishima, K. Hashimoto, *Science* 272 (1996) 704.
- [5] O. Sato, Y. Einaga, A. Fujishima, K. Hashimoto, *Inorg. Chem.* 38 (1999) 4405.
- [6] A. Bleuzen, C. Lomenech, V. Escax, F. Villain, F. Varret, C. Cartier dit Moulin, M. Verdagner, *J. Am. Chem. Soc.* 122 (2000) 6648.
- [7] Y. Morimoto, M. Hanawa, Y. Ohishi, K. Kato, M. Takata, A. Kuriki, E. Nishibori, M. Sakata, S.-I. Ohkoshi, H. Tokoro, K. Hashimoto, *Phys. Rev. B* 68 (2003) 144106.
- [8] N. Shimamoto, S.-I. Ohkoshi, O. Sato, K. Hashimoto, *Inorg. Chem.* 41 (2002) 678.
- [9] V. Ksenofontov, G. Levchenko, S. Reiman, P. Gütllich, A. Bleuzen, V. Escax, M. Verdagner, *Phys. Rev. B* 68 (2003) 24415.

¹ The gap gives rise to an expression of the χT product where g is the Zeeman factor of the complex: $\chi T = (3/4)(g^2/3 + \exp(-\Delta/kT))$.

- [10] E. Corodano, M.C. Gimenez-Lopez, G. Levchenko, F.M. Romero, V. Garcia-Baonza, A. Milner, M. Paz-Pasternak, *J. Am. Chem. Soc.* 127 (2005) 4580.
- [11] O. Sato, T. Iyoda, A. Fujishima, K. Hashimoto, *Science* 271 (1996) 49.
- [12] S.-I. Ohkoshi, H. Tokoro, T. Hozumi, K. Hashimoto, C. Mathonière, I. Bord, G. Rombaut, M. Verelst, F. Villain, C. Cartier dit Moulin, *J. Am. Chem. Soc.* 128 (2006) 270.
- [13] J.M. Herrera, V. Marvaud, M. Verdaguer, J. Marrot, M. Kalisz, C. Mathonière, *Angew. Chem., Int. Ed.* 43 (2004) 5648.
- [14] Y. Arimoto, S.-I. Ohkoshi, Z.J. Zhong, H. Seino, Y. Mizobe, K. Hashimoto, *J. Am. Chem. Soc.* 125 (2003) 9240.
- [15] T. Hozumi, K. Hashimoto, S.-I. Ohkoshi, *J. Am. Chem. Soc.* 127 (2005) 3864.
- [16] K.R. Dunbar, R.A. Heintz, *Prog. Inorg. Chem.* 45 (1997) 283.
- [17] L.M. Beltran, J.F. Long, *Acc. Chem. Res.* 38 (2005) 325.
- [18] M. Ohba, H. Okawa, N. Fukita, Y. Hashimoto, *J. Am. Chem. Soc.* 119 (1997) 1011.
- [19] M. Verdaguer, A. Bleuzen, V. Marvaud, J. Vaissermann, M. Seuleiman, C. Desplanches, A. Sculler, C. Train, R. Garde, G. Gelly, C. Lomenech, I. Rosenman, P. Veillet, C. Cartier, F. Villain, *Coord. Chem. Rev.* 190–192 (1999) 1023.
- [20] P. Przychodzen, T. Korzeniak, R. Podgajny, B. Sieklucka, *Coord. Chem. Rev.* 250 (2006) 2235.
- [21] G. Rombaut, M. Verelst, S. Golhen, L. Ouahab, C. Mathonière, O. Kahn, *Inorg. Chem.* 40 (2001) 1151.
- [22] C. Mathonière, R. Podgajny, P. Guionneau, C. Labrugère, B. Sieklucka, *Chem. Mater.* 17 (2005) 442.
- [23] J.G. Leipoldt, L.D.C. Bok, P.J. Cilliers, *Z. Anorg. Allg. Chem.* 409 (1974) 3.
- [24] S. Tyagi, B. Hathaway, *J. Chem. Soc., Dalton Trans.* (1984) 2087.
- [25] A. Boutlif, D. Louer, *J. Appl. Crystallogr.* 24 (1991) 987.
- [26] H. Isci, W. Mason, *Inorg. Chim. Acta* 357 (2004) 4065.
- [27] A.B.P. Lever, *Inorganic Electronic Spectroscopy*, second ed. Elsevier, Amsterdam, 1984.
- [28] H. Henning, A. Rehorek, D. Rehorek, P. Thomas, *Inorg. Chim. Acta* 86 (1984) 41.
- [29] X.-D. Ma, T. Hokoyama, T. Hozumi, K. Hashimoto, S.-I. Ohkoshi, *Phys. Rev. B* 72 (2005) 094107.
- [30] T. Korzeniak, K. Stadnicka, M. Rams, B. Sieklucka, *Inorg. Chem.* 43 (2004) 4811.